SECURITY & DEFENCE QUARTERLY

Movement to contact and vanguard UAVs: Strategies for swarm UAV battlefield economics in the era of microwave directed energy weapons

Peter Jonathan Cumpson

pjcumpson@auto617.co.uk

https://orcid.org/0000-0002-7517-0659

Auto617 Ltd., Collingwood Buildings, NE1 1JF, Newcastle upon Tyne, UK

Abstract

This paper examines how the emergence of high-power microwave (HPM)-directed energy weapons alters the economics, tactics, and survivability of small unmanned aerial vehicles (UAVs) operating in contested airspace. The objective is to show that the traditional assumption—namely that a drone swarm must internally communicate and coordinate—does not hold under HPM threat conditions. Instead, a simple movement-to-contact model with a sacrificial vanguard UAV can provide robust early warning to following platforms even when all communications are denied. The study develops a minimal analytical model combining (1) empirical survivability envelopes of HPM systems, (2) simple kinematic geometry for UAV approach and spacing, and (3) probabilistic treatment of vanguard destruction and warning time. Model behaviour is explored across realistic ranges of HPM power, beam width, and UAV cost, requiring no prior assumptions of swarm intelligence. The analysis shows that a single inexpensive vanguard UAV can reliably trigger the adversary's HPM system, providing exploitable warning to UAVs behind it even in complete blackout of communications. This passive signalling effect preserves swarm effectiveness while sharply reducing coordination complexity. Results indicate that low-cost drones can maintain high breakthrough probability against HPM defences when spaced appropriately, and that classical "swarm" behaviour is unnecessary. HPM counter-uncrewed aerial systems inadvertently create a new detectable signature: the microwaves that destroy the vanguard UAV. This cue, not present in kinetic or laser weapons, enables a simplified, robust approach tactic that favours cheap attritable UAVs. Future force design should consider vanguard-based movement-to-contact as a cost-effective alternative to complex autonomous swarming in electromagnetic-contested environments.

Keywords:

unmanned aerial vehicles (UAVs), high-power microwave (HPM) weapons, counter-UAS systems, movement-to-contact tactics, vanguard drone

Article info
Received: 28 November 2025
Revised: 25 April 2026
Accepted: 27 April 2026
Available online: 19 June 2026

Citation: Cumpson, P.J. (2026) 'Movement to contact and vanguard UAVs: Strategies for swarm UAV battlefield economics in the era of microwave directed energy weapons', *Security and Defence Quarterly*, 54(2). doi: 10.35467/sdq/221147.

Introduction

Directed energy weapons (DEWs), such as high power microwave (HPM) systems, have received substantial press attention over the last year. Videos in which a whole swarm of drones fall out of the sky under HPM attack have been very impressive, seemingly offering a solution to swarming tactics that seem to be difficult to counter in other ways.

However, countermeasures are developed against all weapons sooner or later. The question of how swarm (or individual) drones may counter HPM attack (beyond straightforward electromagnetic hardening) has not been addressed in the literature.

Will the advantages of HPM in countering drone swarms survive simple drone countermeasures? How will those countermeasures relate to the unique properties of HPM weapons?

Our research aim in this paper is to consider for the first time *what drone swarms can do to protect themselves by modifying their swarming behaviour*. We shall see that HPM weapons (unlike laser or kinetic weapons) have a particular weakness that is a direct consequence of their strength: their ability to impact simultaneously a large area means that they cannot avoid alerting an even wider area to their presence.

Small Unmanned Aerial Vehicles (UAVs)/Loitering ("Kamikaze") Munitions

Drones or UAVs have become very prominent in the media and on the battlefield. Small uncrewed systems and loitering munitions have moved from niche to ubiquitous, with the Russia–Ukraine war accelerating adoption across regular and irregular forces and normalising first person view (FPV) drones as improvised loitering munitions (Brenner and Ferran, 2024; Hvizda *et al.*, 2025; International Institute for Strategic Studies [IISS], 2024; Watling *et al.*, 2023). Authoritative surveys define loitering munitions as expendable assets combining intelligence, surveillance, and reconnaissance (ISR) and terminal attack, distinct from multi-rotor UAVs that drop ordnance (Brenner and Ferran, 2024), while current policy and strategy analyses emphasise rapid innovation cycles, mass, and electromagnetic warfare (EW) susceptibility observed at scale in Ukraine (Bondar, 2025; Hvizda *et al.*, 2025). Procurement signals echo these trends (e.g. Germany's move to acquire loitering munitions), and global actors are openly pursuing mass production of "suicide drones." Across these sources, a consistent picture emerges: low unit cost and operator-in-the-loop precision drive proliferation; survivability depends on the counter-uncrewed arial systems (C-UAS) environment (things such as EW, kinetic weapons, and DEWs). Despite the rapid progress of artificial intelligence (AI), autonomy beyond short-horizon waypointing remains constrained, with human oversight still central (Bondar, 2025; International Institute for Strategic Studies, 2024).

Military Expectations, Practice, and Doctrine for UAV Swarms

Military interest in UAV swarms stems from their potential to overwhelm traditional air-defence decision loops by exploiting simultaneity, dispersion, and redundancy. Swarming emphasises many-on-few dynamics in which numerous, relatively simple

agents impose disproportionate cost on defenders by saturating sensors, command-and-control (C2), and interceptors while preserving mission outcomes despite attrition (Arquilla and Ronfeldt, 2000). From an engineering perspective, swarms leverage local rules (collision avoidance, goal seeking, and limited neighbourhood awareness) to produce robust collective behaviour without a single point of failure; decades of work on distributed flocking and collective motion provides a theoretical basis for such emergent coordination even with minimal or intermittent communications (Couzin *et al.*, 2002; Reynolds, 1987).

High-power microwave (HPM) directed-energy weapons

Within counter-UAS, HPM DEWs are maturing from decades of NATO/US Department of Defense research on coupling, susceptibility, and hardening into fieldable systems that promise one-to-many effects against swarms (NATO RTO, 2003; NATO Science and Technology Organization (STO), 2010; Reding *et al.*, 2023). Recent demonstrations include Air Force Research Laboratory's (AFRL) THOR engaging multi-drone swarms and industry systems (e.g. Epirus "Leonidas") disabling dozens of UAVs in a single activation, underscoring the potential of wide-area electromagnetic effects versus laser "one-by-one" engagements (AFRL, 2023; Epirus Inc., 2025). At the same time, government assessments note enduring transition challenges—power/aperture scaling, repeatability and characterisation of lethality/safe severities, fratricide/electromagnetic compatibility (EMC), logistics, and Concept-of-Operations (CONOPS) integration—alongside policy and acquisition hurdles that can slow operationalisation despite increasing investment. For small UAVs specifically, the literature highlights vulnerable coupling paths (power electronics, flight-control signal paths, and radio-frequency [RF] front-ends), the importance of platform hardening, and the prospect that HPM becomes a central layer in layered C-UAS architectures where cost-per-shot and swarm coverage dominate (NATO Science and Technology Organization (STO), 2010).

The United Kingdom is developing a sovereign RF DEW (RF-DEW) capability for counter-UAS missions. The current demonstrator, led by a Thales, UK-headed industry consortium under the Ministry of Defence's "Team HERSA" initiative, has undergone live trials with the British army. Public reporting indicates effective engagement of small UAVs at ranges of approximately 1 km, with near-instant effects and a cost-per-shot on the order of pence, highlighting its potential as a low-cost complement to the existing short-range air defence systems. The demonstrator will not enter service in its current form; instead, it is intended to inform future RF-DEW requirements, doctrine, and procurement pathways as part of a layered UK air-defence architecture integrating kinetic, electronic-warfare, laser, and RF-based effectors.

China has demonstrated rapid progress in the development and fielding of HPM systems tailored for counter-UAS roles. These systems emphasise mobility, rapid engagement of small UAS, and integration within multi-layered air-defence architectures. The FK-4000, developed by the China Aerospace Science and Technology Corporation (CASC), exemplifies a long-range mobile HPM system. Public reports indicate an effective range on the order of 3 km with the ability to disable light drones in less than one second. Defence major Norinco's Hurricane-3000 is optimised for drone-swarm engagement and sustained operations. It reportedly engages effectively within 3km, with radar/sensor detection to ~6 km and optical tracking to ~4 km.

Beyond flagship systems, at least three additional vehicle-mounted HPM variants have been shown publicly in China, including integrations on 8x8 light armoured vehicles and heavy trucks (e.g. Shacman SX2400/2500-series) with mast-mounted surveillance radars and articulating microwave emitters. These illustrate a trend towards a *family* of HPM systems covering different mobility, power, and sensor-integration trade-offs—supporting roles from fixed-site defence and convoy protection to rapidly re-deployable tactical missions.

HPM for counter-swarm defence: Why this leads to microsecond pulsing

This section summarises the physical and engineering reasons why modern solid-state HPM architectures tend to operate with longer pulse envelopes than classic 1950s tube-based devices, and why those longer pulses are advantageous when the mission is to disable large numbers of small UASs (swarms). There is little information in the public domain about pulse lengths used by the HPM weapons described above, but their counter-swarm rationale, the use of solid-state electronics and phased-arrays, suggests a trend towards microsecond and longer pulse widths.

Tube-based pulsed-power HPM sources (vircators, relativistic magnetrons, Marx-driven magnetrons, etc.) produce extremely high instantaneous power over very short durations (typical pulse widths in the nanosecond to microsecond range) with very low duty cycles and therefore low average power. By contrast, solid-state power amplifiers such as gallium nitride–laterally diffused metal oxide semiconductor (GaN-LDMOS) phased arrays, trade peak instantaneous power for the ability to sustain high average power and high repetition rate. Practically, semiconductor devices are constrained by device breakdown, thermal limits, and drive/capacitor technology: they are far more capable of delivering microsecond to millisecond envelopes at substantial average power than of producing single-shot gigawatt (GW)-class nanosecond spikes.

Phased-array architectures rely on coherent control of many transmitter/receiver modules. Effective electronic steering, nulling, and adaptive spatial shaping require a waveform with sufficient temporal extent to apply and maintain the desired phase relationships across the aperture, to track moving targets and to sweep or dwell over a volume. Ultra-short isolated spikes provide little time for adaptive beam manipulation; longer pulses (or trains of pulses) enable continuous steering, adaptive nulling, and quasi-continuous-wave (CW) illumination that better support area coverage. Hence, there is a general trend towards longer (1–10 μs), steerable pulses in HPM hardware.

Mechanism of effect against small UAVs

The vulnerability mechanisms for small UAVs include: upset of digital electronics, collapse or disturbance of power rails and regulators, failure or desynchronisation of radio/telemetry links, and thermal or cumulative stress on power-electronics. Many of these mechanisms are cumulative or time-dependent: sustained or repeated energy deposition is more likely to produce widespread malfunction across many heterogeneous platforms than isolated sub-nanosecond strikes, unless those strikes reach exceptionally high peak fields. Consequently, longer pulses increase the probability of producing functional degradation across an ensemble of devices. From an engineering-logistics perspective, long pulses yielding high average power are the natural operating mode for fieldable mobile systems.

Practical HPM detection devices

The open literature already documents practical, fieldable concepts for detecting HPM events with modest hardware. Adami *et al.* (2014a) describe both the limits of early broadband diode detectors and a demonstrator system based on modern logarithmic detector integrated circuits (ICs) and broadband spiral antennas with >60dB dynamic range, capable of extracting pulse amplitude, width, repetition frequency, and count across roughly 0.5GHz to 8GHz, with robustness tests reported to ~kV/m field levels (Adami *et al.*, 2011). Their survey also records multiple off-the-shelf or prototype detectors (e.g. QinetiQ *Canary*, Market Central "microwave microphone," and a Netherlands Organisation for Applied Scientific Research developed unit) and publishes indicative threshold bands: on the order of ~100V/m for continuous wave (CW) upsets and ~10^3V/m for pulsed/multi-cycle events, with steeper single-pulse transients in the kV/m range (Adami *et al.*, 2011).

A follow-on chapter by the same group, "HPM detector with extended detection features" (Adami *et al.*, 2014a), details a multi-channel approach (four polarisation-independent antennas and logarithmic detector chains) that augments simple thresholding with coarse direction finding and pulse parameterisation, further underscoring that HPM engagements are electronically conspicuous even to relatively austere sensors. Complementing these engineering demonstrations, a recent review in *IEEE Transactions on Instrumentation and Measurement* synthesises HPM classification, sources, and detection techniques (including operation in strong electromagnetic [EM] environments), reinforcing that robust, low-SWaP HPM detection is technically routine, rather than speculative (Jia *et al.*, 2024).

Taken together, these sources support the central premise of this paper: HPM use against one UAV typically produces signatures detectable by others nearby, enabling threshold-based warning and autonomous dispersion with minimal sensor sophistication.

In summary, the detection problem considered here is not precision HPM metrology but threshold warning. The relevant question is therefore whether a low-mass detector can trigger before destructive field levels are reached, and whether the resulting warning interval is tactically exploitable.

Models and magnitudes of HPM threat

We begin to model the effect of HPM weapons on UAV systems. This requires some routine consideration of beam geometry and potential power and field delivered by such systems. This is necessarily an approximate, given the variety of systems discussed above and the fact that many of their parameters and performance characteristics are not in the public domain. The model is therefore best interpreted as a sensitivity framework, rather than as a prediction for any specific classified HPM system: the qualitative conclusion is robust when the detector trip field is below the destructive field and when the interval between vanguard engagement and exposure of main body permits non-negligible lateral dispersion.

Proposed addition: model scope and assumptions

The analytical model used in this paper is intended as a deliberately simple, transparent framework for exploring the tactical consequences of HPM detectability, rather than as a

http://doi.org/10.35467/sdq/221147

Table 1. Assumptions made in the models developed in this paper, and consequential limitations.

Assumption	Baseline treatment in this paper	Implication/limitation
Far-field/fixed beam geometry	Uses inverse-distance electric-field scaling and fixed beam divergence for order-of-magnitude estimates	Appropriate for transparent scaling arguments, but not a substitute for system-specific electromagnetic simulation or measured beam maps
Representative HPM thresholds	Uses public-domain threshold bands for detector trip, electronic upset, and destructive effects	Absolute ranges are illustrative; conclusions should be interpreted through threshold ratios and sensitivity to parameter ranges
UAV motion and spacing	Models closure speed, vanguard-to-main-body spacing, and lateral dispersion using simple kinematics	Captures timing and geometry of warning, but omits detailed flight dynamics, autonomy limits, and airframe-specific manoeuvre performance
Detection mechanism	Treats the onboard HPM sensor as a threshold-warning device, rather than a calibrated field-strength instrument	Sufficient for triggering autonomous evasive manoeuvres; not intended for precision source characterisation or localisation
Defender behaviour	Baseline scenario assumes, the defender may engage the vanguard with HPM to protect the defended asset	Adaptive layered defence may instead use guns, interceptor UAVs, missiles, or EW against the vanguard; this is a boundary condition and motivates multi-axis extensions
Swarm coordination	Assumes no inter-UAV communication is required after HPM detection	Highlights robustness under communications denial, but does not preclude more sophisticated coordinated tactics where communications survive

high-fidelity prediction for any specific classified weapon system. The following assumptions define the scope of the model and clarify how the illustrative parameter values should be interpreted. They also identify the main limitations and the variables most suitable for later sensitivity analysis or hardware-in-the-loop validation.

This framing should be read as a sensitivity framework: the central qualitative result is strongest where the detector trip threshold is materially below the destructive field threshold and where the warning interval permits non-negligible lateral dispersion before the main body enters the lethal engagement volume.

Beam width and solid angle of HPM systems

For a circular aperture, the half-power beam width (HPBW) in degrees may be approximated by

$$\mathrm{HPBW} \approx 70^{\circ}\frac{\lambda}{D}$$

where D is the effective aperture diameter and λ is the wavelength. For a rotationally symmetric beam of full-angle HPBW θ, the solid angle is

$$\Omega = 2\pi\left(1-\cos\frac{\theta}{2}\right),$$

and the corresponding antenna gain (assuming high efficiency) is approximately

$$G \approx \frac{4\pi}{\Omega}.$$

Common reference values (circular beam) are set out in Table 2.

In typical use cases: narrow beams (<10°) maximise field intensity at range (hard-kill, single-UAV engagement), while wide beams (30°–60°) enable "blanket" effects suited to swarm defeat at reduced peak field strength.

Range scaling of HPM intensity and electric field

Assuming far-field conditions and a fixed beam divergence (solid angle Ω), the on-axis (power) intensity and electric field scale with range r are as follows. The radiated power spreads over a spherical sector of area Ωr^2, giving an approximate power flux density,

$$S(r) \approx \frac{P_{tx}}{\Omega r^2},$$

where P_{tx} is the transmitted RF power. Thus, the intensity falls as $1/r^2$.

The electric field strength is related to the intensity by

$$S = \frac{E^2}{2\eta_0},$$

where $\eta_0 \approx 377\ \Omega$ is the impedance of free space. Substituting this into the expression above yields

$$E(r) \approx \sqrt{\frac{2\eta_0 P_{tx}}{\Omega}}\frac{1}{r},$$

so the peak electric field strength falls approximately as $1/r$.

Table 2. Solid angle and antenna gain for selected HPM transmission HPBW (a measure of how broad is the beam).

Full-angle HPBW (θ)	Ω (sr)	G (dBi)
2°	1.0×10^{-3}	≈ 30
5°	6.0×10^{-3}	≈ 27
10°	2.4×10^{-2}	≈ 24
30°	2.14×10^{-1}	≈ 15
60°	8.4×10^{-1}	≈ 9.7

In practical terms, this means that while total energy delivered per unit area drops rapidly with distance, the electric field (which governs induced voltages and the likelihood of electronic upset or breakdown) decays more slowly. A wider beam (larger Ω) reduces on-axis field strength at a given range, whereas narrowing the beam (smaller Ω) increases it. These relations assume a constant beam divergence; near-field effects, side-lobes, and electronically steered changes in Ω can introduce deviations.

Neon lamp microwave detection: trip field and warning range

For the purposes of this analysis, we consider the simplest possible HPM detector. A very simple and lightweight method of detecting an HPM strike is to fit UAV with a miniature gas-discharge (e.g. neon) indicator lamp connected, so that its leads act as a small dipole antenna. When exposed to a sufficiently strong microwave electric field, the gas within the lamp undergoes electrical breakdown, and atoms ionise, recombine with electrons and emit a brief flash, which can be detected optically onboard. Indeed, it is easily detected through electromagnetic screening, such as a copper mesh that may be used to "harden" the main body of UAV to HPM attack. This simple gas-discharge device provides a low-cost threshold sensor for HPM exposure.

For a small neon bulb with a strike voltage V_{th} of around 100V, the effective electric field threshold depends on dipole length (formed by lamp leads). Typical order-of-magnitude values are as follows:

$$E_{th} \approx \begin{cases} 3\ \text{kV/m} & \text{for a 6 cm dipole,} \\ 6\ \text{kV/m} & \text{for a 3 cm dipole,} \\ 12\ \text{kV/m} & \text{for a 1.5 cm dipole,} \end{cases}$$

In the radiating far field, assuming a fixed beam divergence (solid angle Ω), the on-axis electric field of the HPM pulse scales as $E(r) \propto 1/r$. The approximate warning range, r_{trip} at which the detector triggers is as follows:

$$r_{\text{trip}} = \sqrt{\frac{2\eta_0 P_{\text{tx}}}{\Omega E_{\text{th}}^2}}.$$

This shows that halving the electric-field threshold doubles the warning distance, and that narrower beams (smaller Ω) reduce the time available for evasive action.

As an illustration, for a plausible peak effective isotropic radiated power, P_{EIRP}, in the range;

$$P_{EIRP} \sim 10^{10} - 10^{12}\ \text{W}$$

for modern HPM counter-UAS systems (US Government Accountability Office (GAO), 2023), a 6-cm neon-dipole detector may trigger at ranges of order of hundreds of metres to multiple kilometres. Shorter dipoles (e.g. 1.5 cm), while compact, raise the trip threshold and therefore reduce warning distance. Pulsed HPM also increases the likelihood of ionization, because repeated peaks provide multiple opportunities for the strike voltage to be exceeded.

This form of detector is therefore most useful for early warning and evasive manoeuvre initiation, rather than for precise field measurement. Multiple lamps of different dipole lengths and orientations are employed to improve frequency and polarisation coverage.

We now compare this detection range with the UAV "kill" range.

Destruction thresholds and warning distance for HPM effects

Open sources do not provide a single universal "kill field" for small UAVs; instead, thresholds vary with frequency, pulse width, beam width, aspect, and coupling path ("front-door" *via* antennas *vs*. "back-door" *via* wiring and seams). Nonetheless, the literature and test practice indicate a consistent banding: (i) *upset/loss-of-control* can begin from a few hundred volts per metre into a low thousands of volts per metre regime for vulnerable configurations; and (ii) *permanent damage/burnout* to susceptible electronics is often discussed around 10 to 25 kV/m on-target fields for short pulses, depending on coupling (Chaari, 2021; Karcz *et al.*, 2023).

For comparison, baseline radiated-immunity requirements for military and automotive electronics (not HPM, but indicative of design targets) are typically specified at about 200V/m CW over wide bands (with higher levels in certain radar sub-bands), meaning civilian commercial off-the-shelf (COTS) avionics and consumer-grade drones—often designed to much lower electromagnetic compatibility (EMC) levels—will generally show *lower* upset/damage thresholds than hardened platforms (International Organization for Standardization (ISO), 2021; US Department of Defense, 2015). Hardened small UAVs employing bonding, shielding, filtering, and partitioning can shift upset upward (and extend destruction distance), but are *not* invulnerable to multi-kV/m HPM environments (GAO, 2023).

Assuming far-field conditions and fixed beam divergence, the on-axis electric field scales as $E(r) \propto 1/r$.

Using effective isotropic radiated power P_{EIRP} (or P_{tx} and solid angle Ω), the approximate trip/destruction range for a threshold E_{th}, is

$$r_{\mathrm{th}} - \frac{\sqrt{\eta_0 P_{\mathrm{EIRP}} / (2\pi)}}{E_{\mathrm{th}}} = \sqrt{\frac{2\eta_0 P_{\mathrm{tx}}}{\Omega E_{\mathrm{th}}^2}}, \quad \eta_0 \approx 377\Omega.$$

Approximate, illustrative ranges: Using the equation above, representative thresholds, and peak P_{EIRP} give:

Table 3. Electric Field thresholds E_{th}, and the distances from the HPM weapon at which such fields can be achieved given three possible effective isotropic radiated powers, P_{EIRP}.

E_{th}	$P_{\mathrm{EIRP}} = 10^{10}$ W	10^{11} W	10^{12} W
3 kV/m	258 m	0.82 km	2.58 km
6 kV/m	129 m	0.41 km	1.29 km
12 kV/m	64.6 m	0.20 km	0.65 km
20 kV/m	38.7 m	0.12 km	0.39 km

These bands are consistent with lower thresholds (shorter destruction distances) for unprotected "civilian" quadcopters; and higher thresholds (longer distances) for hardened military-class small UAVs. This is also consistent with programmatic reporting that HPM CUAS systems aim to deliver disruptive or destructive effects within sub-kilometre to kilometre-class ranges, depending on beam width and target set (GAO, 2023; Karcz *et al.*, 2023).

Warning Capability of a Neon Lamp HPM Detector

A key question for survivability is whether a simple neon lamp-based detector provides sufficient early warning for a small UAV to take evasive action before experiencing disruptive or destructive HPM field strengths. Using peak effective isotropic radiated powers in the range $P_{EIRP} \sim 10^{10} - 10^{12}$ W, consistent with publicly discussed HPM counter-UAS concepts (GAO, 2023), the 6-cm neon detector would typically provide warning at distances from several hundred metres to multiple kilometres, depending on system parameters. The corresponding time margin for evasive action (e.g. rapid alteration of trajectory, attitude, or speed) would be on the order of several seconds to over one minute for small UAVs travelling at 30–50 m/s, subject to propagation effects, beam pointing, polarisation alignment, and whether the UAV is illuminated by main lobe or side lobe.

This analysis suggests that, in many engagements, a lightweight neon-based detector can provide meaningful early warning against HPM attack, particularly for wide-beam systems or initial detection of a scanning main lobe. Performance can be enhanced by using multiple orthogonally mounted lamps of differing lengths to reduce polarisation and frequency sensitivity, and by linking detection to a predefined automatic evasive-manoeuvre protocol.

Implications of HPM detectability: Stochastic dispersion and the "wasp swarm" effect

Detection of an imminent HPM activation by a simple threshold sensor (e.g. a neon lamp dipole) does not itself harden a UAV platform, but it can materially change the attacker–defender engagement geometry by inducing an immediate, local, and *autonomous* avoidance response. Even in the absence of inter-vehicle communication or coordinated command, such individualised, randomised evasive manoeuvres rapidly reduce target areal density and thereby decrease the probability that a subsequent narrowly directed HPM pulse will illuminate multiple surviving vehicles. This phenomenon can be understood formally, but is intuitively captured by the "wasp swarm" analogy: Dispersing a compact cluster into many independent trajectories makes it significantly harder to neutralise the threat in subsequent attempts, even though each individual element remains vulnerable.

A simple probabilistic model

Consider a swarm of small UAVs approaching a defended sector. At range r, the HPM emitter subtends an irradiated footprint on the target plane of area

$$A(r) = \Omega r^2,$$

where Ω is the beam solid angle, as introduced in the section above. Let the initial mean areal density of UAVs in the swarm be λ_0 (vehicles per m^2), typically a good deal less

than unity. The number of vehicles illuminated at that instant is (approximately) Poisson-distributed with mean,

$$\mathbb{E}[N_0] = \lambda_0 A(r)$$

Suppose the HPM activation destroys each illuminated vehicle independently with probability p_{kill}. The expected number of immediate survivors within the illuminated footprint is therefore

$$\mathbb{E}[S_0] = \mathbb{E}[N_0](1 - p_{\text{kill}})$$

Assume that each surviving vehicle executes an autonomous, randomised evasive manoeuvre immediately upon detection. We model this as isotropic lateral dispersion at effective sideways speed v_{disp} sustained for a delay Δt before any subsequent HPM pulse can be delivered. After this interval, the survivors occupy, on average, an area of the order

$$A_{\text{after}} \approx \pi(R_0 + v_{\text{disp}}\Delta\text{t})^2,$$

where R_0 is the initial effective radius of the illuminated group (so that $\text{A}(r) \approx \pi R_0^2$). The mean areal density after dispersion, λ_{after}, is approximately

$$\lambda_{\text{after}} \approx \frac{\mathbb{E}[S_0]}{A_{\text{after}}} = \frac{\lambda_0 A(r)(1 - p_{\text{kill}})}{\pi\left(R_0 + v_{\text{disp}}\Delta t\right)^2}.$$

A subsequent narrow beam pulse at the same range again subtends area $A(r)$, so the expected number of vehicles re-illuminated is $\lambda_{\text{after}}A(r)$. The ratio of the expected re-engagement count to the initial count is therefore

$$\mathcal{F} = (1 - p_{\text{kill}})\frac{R_0^2}{\left(R_0 + v_{\text{disp}}\Delta t\right)^2}.$$

This expression highlights two multiplicative effects that both reduce follow-on engagement effectiveness: (i) incomplete initial kills $(1 - p_{\text{kill}})$, and (ii) geometric dilution of areal density because of dispersion. Two immediate implications follow:

1. *First-shot effectiveness is critical*. Unless p_{kill} is close to unity, a single narrowly focused HPM engagement is unlikely to remove the swarm as a threat. Any surviving vehicles disperse and become significantly harder to re-acquire within a narrow beam on subsequent pulses.

2. *Even modest lateral dispersion is highly effective*. For example, if R_0 = 20 m and surviving UAVs achieve lateral offsets of $v_{\text{disp}}\Delta t$ = 40 m before the next pulse, the dilution factor from dispersion alone is $(20/(20 + 40))^2 \approx 1/9$, viz. roughly an order-of-magnitude reduction in target density, even before accounting for initial kills.

This directly parallels the "wasp swarm" analogy: dispersing a tight cluster of individually fragile agents transforms a single-direction defensive problem into a multi-vector one. Even without communication between UAVs, random autonomous dispersion significantly increases the defender's resource and time requirements for neutralisation.

Doctrinal consequences

To counter a detect-and-disperse swarm effectively, a defender must consider one or more of the following:

1. Achieving sufficiently high p_{kill} on the first pulse through increased P_{EIRP}, multiple simultaneous beams, or optimised beam shaping.

2. Employing a wider beam (larger Ω) to maintain coverage of the dispersed cloud, accepting lower peak field strength per target.

3. Using multi-modal, layered effects (e.g. HPM combined with laser or kinetic interceptors) or multiple spatially separated emitters to limit the benefits of dispersion.

The above model omits additional factors, such as near-field effects, ground reflections, polarisation mismatch (relevant for dipole-type detectors), and potential partial degradation of flight control following initial exposure. These effects should be incorporated in higher-fidelity simulation or hardware-in-the-loop trials.

Worked numerical example

To illustrate orders of magnitude, consider an initial compact group with effective radius $R_0 = 20$ m (so $A(r) \approx \pi R_0^2 \approx 1{,}257$ m^2) and mean areal density $\lambda_0 = 0.032$ m^{-2}, yielding an expected initial count of forty UAVs

$$\mathbb{E}[N_0] = \lambda_0 \pi R_0^2 \approx 40.$$

Assume that the first HPM pulse achieves per-vehicle kill probability $p_{\text{kill}} = 0.6$, leaving

$$\mathbb{E}[S_0] = \mathbb{E}[N_0](1 - p_{\text{kill}}) \approx 16$$

immediate survivors within the footprint. Suppose each survivor executes an autonomous lateral evasion with effective sideways speed $v_{\text{disp}} = 20$ m/s and there is a $\Delta t = 2$ s interval before a possible follow-up pulse, giving a lateral offset $v_{\text{disp}}\,\Delta t = 40$ m. The post-dispersion effective area is then

$$A_{\text{after}} \approx \pi(R_0 + v_{\text{disp}}\Delta t)^2 = \pi 60^2 \approx 11{,}310 \text{ m}^2,$$

and the resulting mean areal density becomes

$$\lambda_{\text{after}} = \frac{\mathbb{E}[S_0]}{A_{\text{after}}} \approx \frac{16}{11{,}310} \approx 1.4 \times 10^{-3} \text{ m}^{-2}$$

If a subsequent narrow beam again subtends area $A(r) \approx \pi R_0^2$ at the same range, the expected number re-illuminated on the second pulse is

$$\mathbb{E}[N_1] = \lambda_{\text{after}} A(r) \approx (1.4 \times 10^{-3}) \times 1{,}257 \approx 1.8,$$

viz. a reduction from ≈ 40 initially illuminated vehicles to fewer than two on the next pulse, even before considering any further time for additional dispersion. The governing factor is the dilution ratio

$$\mathcal{F} = (1 - p_{\text{kill}}) \frac{R_0^2}{\left(R_0 + v_{\text{disp}}\Delta t\right)^2} = 0.4 \times \left(\frac{20}{60}\right)^2 \approx 0.044,$$

which here implies roughly a 95% reduction in expected re-engagement count between the first and second pulses. Modest changes in p_{kill}, v_{disp}, or Δt map directly to this ratio and can be used as design or doctrinal tuning parameters.

Biological analogy and doctrinal relevance

The "wasp swarm" analogy is a useful, intuitively accessible framing for dispersion dynamics. In collective animal motion, brief local rules (repulsion/avoidance, heading change, and speed adjustment) generate rapid spatial de-correlation and group reconfiguration without any global communication (Couzin *et al.*, 2002; Reynolds, 1987). In military studies, swarming has long been analysed as a many-on-few paradigm in which distributed, loosely coupled agents exploit simultaneity, manoeuvre, and geometry rather than persistent communications (Arquilla and Ronfeldt, 2000). By analogy, threshold-triggered *autonomous* dispersion in UAV swarms—without inter-vehicle messaging—achieves the operational effect of transforming a dense, beam-vulnerable cluster into a sparse, multi-vector set of trajectories within a few seconds. This increases the defender's resource burden for follow-on engagements (wider beams, multi-beam simultaneity, or cross-domain layering), consistent with the general doctrine that defeating swarms often requires early, broad-pattern effects or near-simultaneous multi-axis fires rather than sequential, narrow-beam re-attacks (Arquilla and Ronfeldt, 2000).

Much of the literature on UAV swarming focuses on inter-vehicle communications and distributed algorithms for formation, task allocation, and resilience, but these same RF links create obvious vulnerability vectors: exposed antennas, radios and power electronics provide coupling paths for jamming, spoofing, and directed-energy effects and significantly raise the platform's EM signature compared with a strictly stand-alone loitering munition. Yet detector demonstrations from Fraunhofer, TNO, and others show that small, low-mass HPM warning/detection packages are technically plausible. We have shown that this would materially change the attacker–defender calculus, even without inter-UAV communication. This then raises the question of what is the best strategy for UAV deployment under such conditions. We can draw an analogy with the doctrine of "movement to contact (MTC)."

Movement to Contact

Movement to contact is an offensive task conducted to develop the situation and establish or regain contact with the enemy when the tactical picture is incomplete (Headquarters, Department of the Army, 2012, 2023). Its logic is to preserve the freedom of action of the main body by ensuring that first contact occurs with a smaller, purpose-organised element that can report, fix, and set conditions for decisive action by follow-on forces (Headquarters, Department of the US Army, 2023).

Doctrinal fundamentals of MTC include: (i) focusing all efforts on finding the enemy; (ii) *making initial contact with the smallest force possible*, consistent with protecting the force; (iii) using small, mobile, self-contained forward elements to avoid decisive engagement of the main body on terrain of the enemy's choosing; (iv) task-organising and employing movement formations to deploy and attack rapidly in any direction; (v) keeping subordinate forces within supporting distance; and (vi) maintaining contact once gained (Headquarters, Department of the US Army, 2023). At small-unit level, movement techniques are explicitly designed to enable initial contact by the smallest feasible element so that leaders can establish a base of fire and maneuver the remainder without first disengaging (Headquarters, Department of the Army, 2024).

Movement to contact commonly uses a security framework of screen/guard/covering elements to provide early warning, develop the situation, and buy time/space for the main body to deploy. Variations such as search-and-attack or cordon-and-search adapt MTC principles to stability or dispersed enemy situations while retaining the core aim of controlled first contact and rapid development of the situation (Headquarters, Department of the Army, 2023, 2024). We observe that MTC is a useful principle to apply to UAV swarming in the presence of HPM weapons.

Vanguard UAV

As we have seen, if an alert mechanism is in place in each UAV, the effectiveness of the HPM in countering a swarm becomes critically dependent on an effective "first shot" to disable most, if not all, of them. Figure 1 shows the schematic approach of a UAV swarm.

In this configuration, as shown in Figure 2, it's possible for the HPM weapon to wait until most, or all, of the UAVs are close enough to be destroyed before initiating HPM pulses.

Thus, an appropriate strategy in the spirit of MTC for the attacker may be to deploy a vanguard UAV in advance of their main swarm, as shown in Figure 3.

The power density at the vanguard UAV is

$$p_1 = \frac{P}{r_1^2}$$

where r_1 is the closest tolerable distance of approach.

This can warn the main UAV swarm if each vehicle has a microwave detector triggered at a threshold power density p_2, where

$$\frac{P}{r_2^2} \geq p_2 .$$

A defender cannot ignore vanguard threat without risk, but need not necessarily answer it with HPM. The vanguard concept is therefore strongest where the attacker can make non-HPM interception costly, saturated, delayed, or uncertain. Importantly, unlike kinetic weapons, the use of HPM cannot prevent some of the directed electromagnetic energy from also alerting the main UAV force to the microwave attack, provided that the spacing behind the vanguard UAV is small enough and the detectors on the following UAVs are sufficiently sensitive.

Figure 1. A swarm of UAVs approaches the HPM weapon. This is a schematic, and not to scale.

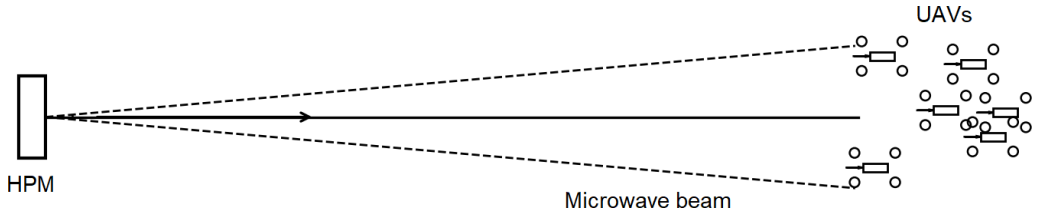

Figure 2. As the swarm comes within the range of HPM, the weapon emits a microwave beam sufficient to destroy some, or all, of the UAV swarm. This is a schematic, and not to scale.

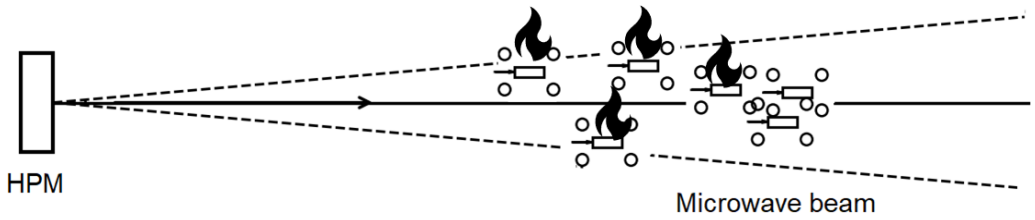

Figure 3. "Vanguard UAV" arrangement in which a single UAV travels far ahead of the main swarm. In this schematic, the HPM is forced to attempt to destroy this nearest UAV. This is a schematic, and not to scale.

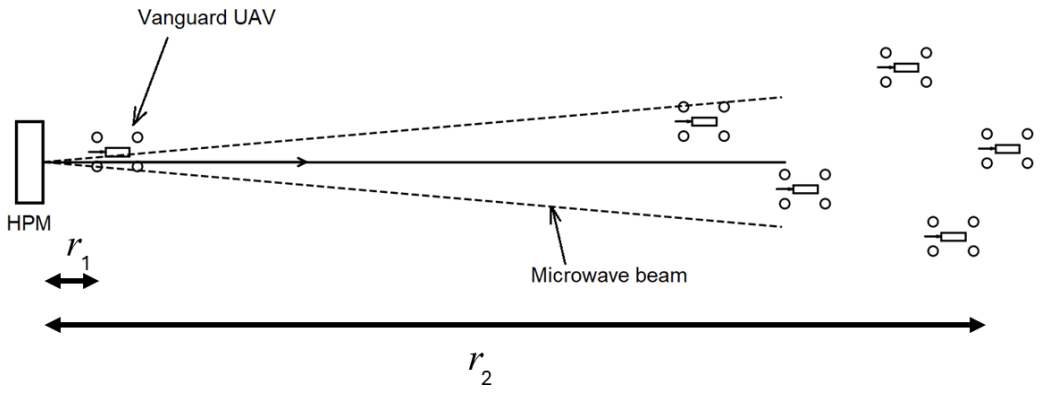

From the two relations above, we obtain

$$r_2 = r_1\sqrt{\frac{p_1}{p_2}},$$

so that if p_2 is 1% of p_1, and the minimum distance the HPM (with its own safety in mind) engage the vanguard UAV is 10 m (say), then the optimum placement of the main UAV force is $r_2 - r_1$, or just <90 m behind the vanguard UAV. This would provide enough time and space for individuals within the main force to disperse before entering any zone where they will be destroyed. Random dispersal, at high speed, might be a sensible choice as soon as HPM is detected, as shown in Figure 4.

Vanguard UAVs and the detect-and-disperse trade space

The concept of vanguard UAV places a forward, sacrificial element ahead of the main swarm to force an adversary's HPM emitter to demonstrate its intent and geometry (cf. the movement-to-contact framing in the section of that title above). If the vanguard UAV compels the defender to fire in order to protect defended assets, the resulting emission will likely destroy the vanguard UAV but risks triggering threshold detectors carried by the follower UAVs; those detectors in turn can initiate autonomous evasive responses that rapidly dilute the areal density of the swarm (dispersion).

In summary, the vanguard concept converts HPM engagement from a hidden terminal event into an observable tactical signal. Its value is greatest where the defender must either reveal the HPM layer early or expend alternative defensive resources against cheap forward probes.

http://doi.org/10.35467/sdq/221147

Figure 4. Result of the configuration shown in Figure 3. The vanguard UAV is destroyed, but each of those in the main swarm detects microwave attack and scatters, very likely out of the solid angle of the beam. This is a schematic, and not to scale.

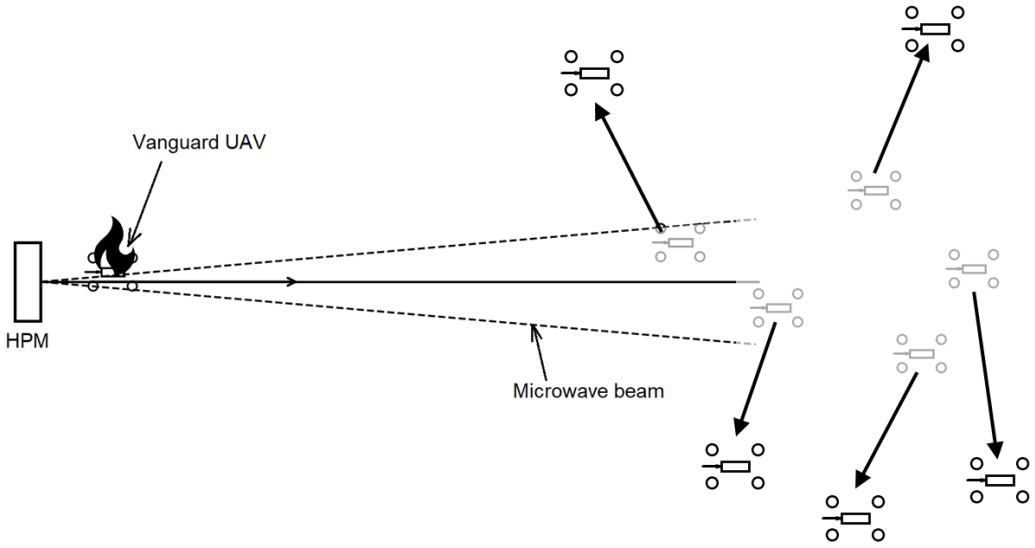

Quantitative example: geometric and temporal margins

For concreteness, we adopt representative (publicly discussed and internally modelled) values: a neon lamp trip threshold for a ~6 cm dipole of

$$E_2 \approx 3 \text{ kV/m}$$

and an illustrative destructive threshold for small UAV electronics of

$$E_1 \approx 15 \text{ kV/m}$$

so that $E_{dest}/E_M \approx 5$ (cf. GAO, 2023). Using the far-field effective isotropic radiated power (EIRP) formulation as defined above, the trip and destructive distances scale with inverse field and thus satisfy

$$\frac{r_2}{r_1} = \frac{E_1}{E_2} \approx 5,$$

independent of EIRP; numerical values, however, do depend on effective radiated power. Table 4 presents worked ranges and time margins for three example peak EIRP envelopes commonly used in HPM order-of-magnitude reasoning (10^{10}, 10^{11}, and 10^{12} W). The time margins shown assume radial closure speeds of v_{uav} = 30 m/s and 50 m/s, respectively.

These examples show that, for plausible EIRP envelopes, the neon (or other) detector can provide an order-of-magnitude spatial margin between detection and destructive field levels. Converting that margin to time yields conservative windows ranging from a few seconds to many tens of seconds depending chiefly on emitter power and platform speed. Such time margins are practically useful: even a short automatic lateral manoeuvre or a short-duration reduction in radar/coupling exposure can move a high proportion of the swarm out of the main lobe (see dispersion model below).

Probabilistic dispersion following vanguard revelation

If the vanguard elicits a defensive HPM shot and the main force detectors trigger, survivors execute autonomous, randomised dispersion. The dilution of areal density and its impact on subsequent narrow-beam engagements is readily quantified. Using the notation introduced above, for an initial illuminated effective radius R_0, the area is $A_0 = \pi R_0^2$. The expected initial count is $\mathbb{E}[N_0] = \lambda_0 A_0$. If the first pulse achieves per-vehicle kill probability p_{kill}, the survivors $\mathbb{E}[S_0] = \mathbb{E}[N_0](1 - p_{\text{kill}})$ disperse to an effective radius $R_{\text{after}} = R_0 + v_{\text{disp}}\Delta t$ after delay Δt, producing areal density,

$$\lambda_{\text{after}} \approx \frac{\mathbb{E}[S_0]}{\pi R_{\text{after}}^2} = \frac{\lambda_0 A_0 (1 - p_{\text{kill}})}{\pi R_{\text{after}}^2}.$$

Hence, the expected number re-illuminated by a subsequent narrow beam of the original footprint area is

$$\mathbb{E}[N_1] = \lambda_{\text{after}} A_0 = \mathbb{E}[N_0](1 - p_{\text{kill}}) \frac{R_0^2}{R_{\text{after}}^2}.$$

A worked numerical example (consistent with the above parameters) further highlights the impact. Let R_0 = 20 m, initial expected count $\mathbb{E}[N_0]$ = 40, effective sideways dispersion speed v_{disp} = 20 m/s, and take the conservative time margin Δt from the $P_{\text{EIRP}} = 10^{11}$ W row in Table 4 for v_{uav} = 30 m/s ($\Delta t \approx 21.7$ s), then for p_{kill} = 0.6, we obtain

$$R_{\text{after}} = 20 + (20)(21.7) \approx 454 \text{ m},$$

and hence,

$$\mathbb{E}[N_1] \approx 40 \times 0.4 \times \left(\frac{20}{454}\right)^2 \approx 0.31,$$

that is a lower than 50–50 chance of any UAV being illuminated on a subsequent narrow engagement. Even for shorter time margins and more modest lateral speeds, the dilution factor is large: dispersion converts tens of targets into a spatially sparse cloud that is expensive for the defender to re-engage with a narrow solid-angle beam.

Implications for emitter employment and doctrine

Two strategic conclusions follow:

1. *First-pulse lethality must commensurate with dispersion penalty.* If the defender relies on a single, narrow beam, the required first-shot per-vehicle kill probability grows

Table 4. Illustrative trip and destructive ranges (on-axis) and conservative time margins for representative peak EIRP values. $\Delta t = (r_{\text{trip}} - r_{\text{dest}})/v_{\text{uav}}$

P_{EIRP} (W)	r_2 (m)	r_1 (m)	r_2/r_1	Δt(30 m/s) (s)	Δt(50 m/s) (s)
1010	258	51.6	5.0	6.9	4.1
1011	816	163.3	5.0	21.7	13.1
1012	2582	516.4	5.0	69.4	41.3

Note. Distances computed using the far-field EIRP relation; time margin, $\Delta t = (r_{\text{trip}} - r_{\text{dest}})/v_{\text{uav}}$.

rapidly with initial swarm size and expected dispersion. For practical swarm sizes, a defender must either deliver near-unity p_{kill} across the footprint or accept that survivors will persist and disperse.

2. *Alternative emitter options reduce dispersion advantage.* Wider beams (larger **Ω**) that blanket the expected post-dispersion cloud, multiple simultaneous beams, or multiple spatially separated emitters firing near-simultaneously counter the dilution effect, but at increased resource and power cost (or system complexity). Multi-modal integration (HPM plus kinetic or high-energy lasers (HEL) layers) also reduces reliance on a single-system first shot and is doctrinally attractive (GAO, 2023; Karcz *et al.*, 2023).

Operational and experimental recommendations

To operationalise the vanguard UAV approach and validate the numerical trade space, we recommend a combined modelling and test programme:

1. Monte Carlo simulation sweeps over P_{EIRP}, beam HPBW (**Ω**), E_M, E_{dest}, p_{kill}, v_{uav}, and v_{disp} to map survivor distributions and expected re-engagement counts (probabilistic mission-level risk).

2. Radio-frequency chamber and hardware tests to characterise neon trip (or other detector) thresholds across frequency, polarisation, and orientation, and to measure false-positive rates and response latency.

3. Flight tests with surrogate emitters and instrumented UAVs (non-destructive exposures) or high-fidelity hardware-in-the-loop trials to validate timing, dispersion dynamics and the reliability of automatic manoeuvre protocols.

Taken together, these results are likely to strengthen the strategic case for vanguard UAV employment when combined with threshold detectors: a modestly sensitive, low-mass detector provides a demonstrable temporal window that, when exploited by simple autonomous dispersion, materially increases the resource cost to the defender of neutralising the swarm. Conversely, defenders that rely on sequential, narrow-beam engagements will find that dispersion imposes prohibitive re-engagement costs unless they concentrate sufficient first-shot lethality or adopt wider/overlapping engagement geometries.

Adaptive defenders, layered C-UAS, and multi-axis vanguard employment

The baseline vanguard UAV model deliberately isolates the HPM-specific case in which the defender uses microwave engagement against the leading element. In practice, an adaptive defender may employ layered C-UAS fires, including kinetic weapons, laser DEWs, interceptor UAVs, electronic warfare, and HPM, and may attempt to defeat the vanguard without revealing the HPM emitter. This does not invalidate the detect-and-disperse mechanism, but it narrows the conditions under which a single vanguard is sufficient. Against such an adaptive defence, the attacker's problem becomes one of forcing premature commitment of the HPM layer by presenting multiple low-cost probes, simultaneous axes, altitude-separated arrivals, or decoy-vanguard elements. In doctrinal terms, the vanguard should therefore be understood not only as a single sacrificial UAV but as the simplest member of a broader movement-to-contact family of probing elements.

Modelling such multi-axis and layered defence interactions is beyond the scope of the present minimal analytical model, but follows naturally from the same engagement geometry and cost–exchange framework.

Conclusions

High-power microwave systems represent an attractive counter-swarm technology, offering the prospect of disabling multiple UAVs with a single engagement. However, the "wasp swarm" analogy is a useful way to visualise swarm dispersion dynamics and how it may frustrate the destruction of the swarm as a whole. This paper has examined the fundamental field thresholds relevant to small UAV vulnerability, analysed the feasibility of early HPM detection using a lightweight neon lamp threshold sensor, and quantified the tactical implications of autonomous evasive responses triggered by such detection. A simple but robust probabilistic dispersion model is developed, demonstrating that even brief, uncoordinated manoeuvres can rapidly dilute UAV areal density and drastically reduce the effectiveness of subsequent narrow-beam HPM engagements. Analytical and numerical studies further show that, unless near-unity per-vehicle kill probabilities are achieved on the first shot, dispersion imposes severe re-engagement penalties on the defender.

The "vanguard UAV" concept was introduced and formalised as a sacrificial forward probe, capable of eliciting the initial HPM emission and thereby granting the main swarm a tactically valuable time window for dispersion. Results indicate that, for representative detector thresholds (e.g. a 6-cm neon dipole at ~3 kV/m) and destructive field bands (~10–25kV/m), typical warning intervals range from several seconds to tens of seconds on-axis, depending on microwave power and UAV approach speed. These margins provide sufficient opportunity for dispersion to transform a compact, vulnerable swarm into a sparse, multi-vector threat, significantly increasing the defender's resource burden for follow-on engagements. In operational terms, this shifts the defender's requirement towards wide or overlapping beams, multi-emitter simultaneity, or layered effects, rather than repeated narrow-beam shots.

A central strategic insight emerging from this work is that, unlike laser-directed energy or kinetic C-UAS approaches that often neutralise targets without necessarily alerting others, HPM has an intrinsic *self-revealing* characteristic: any emission sufficient to destroy or disrupt one UAV is likely to be detectable by others in the vicinity. The neon lamp detector analysed here is intentionally elementary, and better alternatives have already been demonstrated, yet already offers meaningful early-warning capability. More sensitive, purpose-designed detectors can only strengthen this effect. That a trivial device of negligible mass, cost, and technical sophistication can materially alter the engagement economics suggests that HPM may not constitute the "silver bullet" against UAV swarms that it is sometimes portrayed to be. Rather, HPM employment against swarms is fundamentally a contest of first-shot effectiveness versus dispersion dynamics, with favourable outcomes relying on doctrine, timing, geometry, and combined effects, not HPM alone.

Future work should extend these models to include near-field effects, beam-steering dynamics, coordinated swarm behaviours, and adversarial learning. Hardware-in-the-loop testing and controlled flight trials are recommended to validate timing, survivability, and dispersion behaviours under realistic conditions. The findings herein highlight that low-cost sensing and autonomy can substantially degrade the operational value of HPM in swarm-defence scenarios, and that resilient swarming tactics remain within reach of even modestly equipped actors.

Funding

This research received no external funding.

Data Availability Statement

The data presented in this study is available on request from the author.

Disclosure Statement

No potential conflict of interest was reported by the author. The author read and agreed to the published version of the manuscript.

References

Adami, C., Braun, C., Clemens, P.,Schmidt, H.-U., Suhrke, M., and Taenzer, H.-J. (2011) 'Detection of high power microwaves', in *Future security 2011*. Bonn. Available at: https://publica.fraunhofer.de/bitstreams/9264f0e2-40aa-45d5-bdb9-80f8fd8db45b/download (Accessed: 17 May 2026).

Adami, C., Braun, C., Clemens, P., Jöster, M., Taenzer, H.-J., Schmidt, H.-U. Suhrke ,M. and Taenzer, H.-J. (2014a) *HPM detector with extended detection features*, in Sabath, F. , Mokole, E. (eds.) *Ultra-wideband, short-pulse electromagnetics* 10. New York, NY: : Springer, pp. 345–353. doi: 10.1007/978-1-4614-9500-0_31.

Adami, C., Braun, C., Clemens, P., Joester, M., Ruge, S., Suhrke, M., Schmidt, H.-U. and Taenzer, H.-J. (2014b) *HPM detector system with frequency identification*, Fraunhofer Institute for Technological Trend Analysis (INT). Proc. of the 2014 International Symposium on Electromagnetic Compatibility (EMC Europe 2014), Gothenburg, Sweden, September 1-4 Available at: https://publica.fraunhofer.de/bitstreams/96531286-fdb6-4aff-baa5-ac392f7e7211/download (Accessed: 17 May 2026).

Air Force Research Laboratory (AFRL) (2023) *AFRL conducts swarm technology demonstration (THOR)*, AFRL news release. Available at: https://www.afrl.af.mil/News/Article-Display/Article/3396995/afrl-conducts-swarm-technology-demonstration/ (Accessed: 17 May 2026).

Arquilla, J. and Ronfeldt, D. (2000) *Swarming and the future of conflict*. Santa Monica, CA: RAND Corporation report DB311.

Bondar, K. (2025) *Ukraine's future vision and current capabilities for waging AI-enabled autonomous warfare*, CSIS analysis. Available at: https://www.csis.org/analysis/ukraines-future-vision-and-current-capabilities-waging-ai-enabled-autonomous-warfare (Accessed: 17 May 2026).

Brenner, J. and Ferran, M. (2024) *L-297 loitering munitions*, NATO MSIAC. Available at: https://www.msiac.nato.int/publication/l-297-loitering-munitions/ (Accessed: 17 May 2026).

Chaari, M.Z. (2021) 'High power microwave for knocking out programmable drones', *Security and Defence Quarterly,* 34(2), pp. 68–84, doi: 10.35467/sdq/135068.

Couzin, I.D., Krause, J., James, N.R., Ruxton, G.D. and Franks, N.R. (2002) 'Collective memory and spatial sorting in animal groups', *Journal of Theoretical Biology*, 218(1), pp. 1–11. doi: 10.1006/jtbi.2002.3065.

Epirus Inc. (2025) *Leonidas high-power microwave defeats 49-drone swarm (100% of drones) at live-fire demonstration*, press release. Available at: https://www.epirusinc.com/press-releases/epirus-leonidas-high-power-microwave-defeats-49-drone-swarm-100-of-drones-flown-at-live-fire-demonstration (Accessed: 17 May 2026).

Headquarters, Department of the Army (2012) *ADP 3-90: Offense and defense*, Department of the Army, Washington, DC. Available at: https://www.benning.army.mil/Infantry/199th/2-16/ABOLC/content/pdf/ADP%203-90%20Offense_Defense.pdf (Accessed: 17 May 2026).

Headquarters, Department of the Army (2023) *FM 3-90: Tactics*, Department of the Army, Washington, DC. Available at: https://archive.org/download/fm-3-90-tactics-2023/FM%203-90%20Tactics%202023.pdf (Accessed: 17 May 2026).

Headquarters, Department of the Army (2024) *FM/ATP 3-21.8: Infantry rifle platoon and squad*. Headquarters, Department of the Army, Washington, DC. Available at: https://infantrydrills.com/manuals/fm-atp-3-21-8-infantry-rifle-platoon-squad-2024/ (Accessed: 17 May 2026).

Hvizda, M., Frederick, B., Laufer, A., Evans, A.T., Gunness, K., and Ochmanek, D.A. (2025) *Dispersed, Disguised, and Degradable: The Implications of the Fighting in Ukraine for Future U.S.-Involved Conflicts*. Santa Monica, CA: RAND Corporation report RRA3141-2.

International Institute for Strategic Studies (IISS) (2024) *The military balance 2024*. London: Routledge. doi: 10.4324/9781003485834.

International Organization for Standardization (ISO) (2021) *ISO 11452-2: Road vehicles—Component test methods for electrical disturbances from narrowband radiated electromagnetic energy—Part 2*, International Organization for Standardization. Chemin de Blandonnet 8, CP 401, 1214 Vernier (Geneva) Switzerland.

Jia, L., Wang, Y., Song, Y., Cui, W., Chen, Z. and Wang, R. (2024) 'The detection technology of high-power microwave: A review', *IEEE Transactions on Instrumentation and Measurement*, 73, pp. 1–16. doi: 10.1109/TIM.2024.3472802.

Karcz, K., Sitkiewicz, A., Błaszczyk, J. and Mierczyk, Z. (2023) 'From disruption to destruction: Assessing the impact of high-power microwaves on autonomous vehicles', in *NATO STO meeting proceedings SET-315*. Available at: https://publications.sto.nato.int/. (Accessed: 17 May 2026).

NATO RTO (2003) *Tactical implications of high power microwaves*. Brussels: NATO RTO. doi: 10.14339/RTO-TM-028.

NATO Science and Technology Organization (STO) (2010) *High power microwave threat to infrastructure and military equipment*, technical report. Neuilly-sur-Seine, Paris: NATO Science and Technology Organization (STO). doi: 10.14339/RTO-TR-SCI-132.

Reding, D.F., Blanco, Á.M., De Lucia, A., Regan, L.A. and Bayliss, D. (2023) *Science & technology trends 2023–2043: volume 2*, NATO. Available at: https://web.archive.org/web/20240706122908/https://www.nato.int/nato_static_fl2014/assets/pdf/2023/3/pdf/stt23-vol2.pdf (Accessed: 17 May 2026).

Reynolds, C.W. (1987) 'Flocks, herds, and schools: A distributed behavioral model', in *Proceedings of SIGGRAPH '87*. Maureen C. Stone (Editor), New York City, NY: ACM, pp. 25–34. doi: 10.1145/37401.37406.

US Department of Defense (2015) *MIL-STD-461g: Requirements for the control of electromagnetic interference characteristics of subsystems and equipment*, US DoD. Available at: https://s3vi.ndc.nasa.gov/ssri-kb/static/resources/MIL-STD-461G.pdf (Accessed: 17 May 2026).

US Government Accountability Office (GAO) (2023) *Directed energy weapons: DoD should focus on transition efforts to ease fielding challenges*, GAO-23-105868. Available at: https://www.gao.gov/assets/gao-23-105868.pdf (Accessed: 17 May 2026).

Watling, J. and Reynolds, N. (2023) *Stormbreak: Fighting through Russian defences in Ukraine's 2023 offensive*. London: Royal United Services Institute (RUSI). Available at: https://static.rusi.org/Stormbreak-Special-Report-web-final_0.pdf (Accessed: 17 May 2026).